

CRYSTAL COLLIMATION AT RHIC *

R. P. Fliller III[†], A. Drees, D. Gassner, L. Hammons, G. McIntyre, S. Peggs, D. Trbojevic, BNL, Upton, NY, 11793, V. Biryukov, Y. Chesnokov, V. Terekhov, IHEP, Protvino, Moscow Region

Abstract

For the year 2001 run, a bent crystal was installed in the yellow ring of the Relativistic Heavy Ion Collider (RHIC). The crystal forms the first stage of a two stage collimation system. By aligning the crystal to the beam, halo particles are channeled through the crystal and deflected into a copper scraper. The purpose is to reduce beam halo with greater efficiency than with a scraper alone. In this paper we present the first results from the use of the crystal collimator. We compare the crystal performance under various conditions, such as different particle species, and beta functions.

1 INTRODUCTION

A collimation system for a high energy collider usually consists of movable jaws positioned such that they form the limiting aperture for the beam. These jaws are located at high beta or high dispersion locations to act as transverse or momentum collimators respectively. Often a single jaw is not sufficient for high collimation efficiency because particles with low impact parameters on the jaw can actually cause a larger, more diffuse halo due to scattering within the jaw [1]. To counteract this effect, secondary jaws are placed downstream to intercept these scattered particles.

It should be possible to increase the collimation efficiency by using bent crystal channeling, because a properly aligned crystal will channel the entering particles away from the beam and produce very little halo from scattering. A properly positioned secondary jaw intercepts the channeled particles. This secondary jaw can be placed further away from the beam, reducing scraper induced halo. This paper discusses our experiences with a bent crystal collimator in the yellow ring of the Relativistic Heavy Ion Collider (RHIC).

2 CRYSTAL CHANNELING

Crystal channeling is a phenomena by which ions impinging on a properly aligned crystal will follow the crystal planes [2]. By mechanically bending the crystal, it is possible to give an angular kick to the channeled particles as they will follow the bend of the crystal planes. For proper alignment of the crystal, the beam must be aligned to the crystal planes to an angle less than the critical angle, θ_c . The critical angle is given by

$$\theta_c = \sqrt{\frac{2U(x_c)}{pv}} \quad (1)$$

where p and v are the momentum and velocity of the ion and $U(x_c)$ is the inter-planar potential at the location, x_c , where the ion will enter the electron cloud of the lattice atoms. $U(x_c)$ is approximately 16 eV for silicon. For RHIC energies, $\theta_c = 37 \mu\text{rad}$ at injection and $11 \mu\text{rad}$ at storage energy. At incident angles greater than θ_c the ion will no longer be trapped between the crystal planes and scatters through the crystal as if it were an amorphous solid.

3 LAYOUT

The RHIC crystal collimation system consists of a 5 mm long crystal and a 450 mm long L-shaped copper scraper placed downstream of the PHENIX detector in the the yellow (counter-clockwise) ring. The crystal is an O-shaped silicon crystal with the (110) planes placed at an angle of $465 \mu\text{rad}$ with respect to the normal of the input face (miscut angle, θ_m), and a 0.44 mrad bend angle, θ_b . There are eight PIN diode loss monitors between the crystal and the scraper (the upstream PIN diodes), and four PIN diodes downstream of the scraper (the downstream PIN diodes) to look for scattered particles from the crystal and scraper respectively. In addition, there are two scintillators forming a hodoscope aligned to the crystal surface. Four ion chamber beam loss monitors are located downstream of the scraper as well[3].

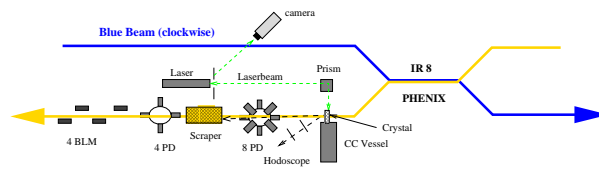


Figure 1: The RHIC Crystal Collimation system

4 SIMULATION

To simulate the action of the crystal in RHIC we used the CATCH (Capture And Transport of CHarged particles in a crystal) code [4] to simulate ion interactions in the crystal, and the K2 code[5] to implement the proton scattering in the copper scraper. Gold ions were assumed to be absorbed by the copper scraper at first impact. For computing speed, a 6×6 matrix was used to track the ions around the ring. Particles are uniformly distributed on the rim of the horizontal phase space ellipse so that only particles that will encounter the crystal are tracked. The distribution in vertical phase space is uniform over a $15\pi \text{ mm-mrad}$ emittance.

* Work performed under the auspices of the U.S. Department of Energy

[†] rfilller@bnl.gov

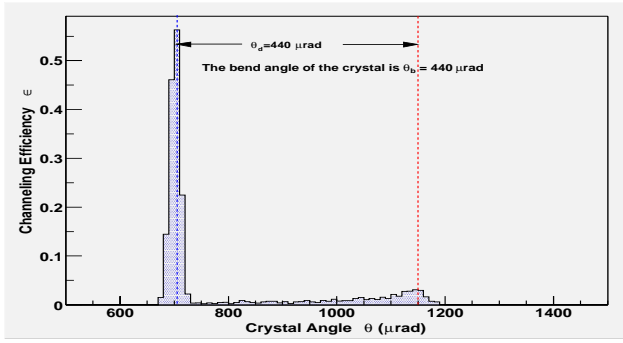


Figure 2: A simulated crystal angular scan.

Figure 2 shows the results of a simulation where the crystal was rotated with respect to a gold beam. The narrower, taller peak corresponds to the angle where the entrance face of the crystal is aligned with the incoming particles. The smaller peak corresponds to the angle where the crystal exit face is aligned to the incoming particles. This separation angle is the bend angle. Ions get channeled at angles other than when the crystal is properly aligned by scattering from a lattice atom into a channel.

5 THE EXPERIMENT

Experiments with the crystal collimator took place during normal gold and polarized proton stores in RHIC. The crystal angle was stepped through a range of angles for a variety of different crystal positions, scraper positions, and lattices. Beam losses were recorded by the PIN diodes, hodoscope, and beam loss monitors. A number of signals from the RHIC experiments were also logged to monitor their local background rates. Table 1 lists the available data samples.

Table 1: Tabulation of Angular Scans

Species	β^* @ IR8	No. of Crystal Angular Scans
Au	5 m	27
Au	2 m	24
Au	1 m	109
p	3 m	119

The $\beta^* = 1$ m is at the PHENIX interaction region only, all the other 5 IRs were kept at $\beta^* = 2$ m.

6 EXPERIMENTAL RESULTS

Figure 3 shows the raw data and the averaged fit data from a typical crystal scan as seen from one of the upstream PIN diodes. Since the PIN diodes see scattered beam, reduction in the signal is evidence for crystal channeling. In this scan the crystal was 32.9 mm away from the beam center as measured by the BPM. The raw data is averaged in $20 \mu\text{rad}$ bins, which corresponds to the resolution of the angular readback, and then fit.

The fit function is given by

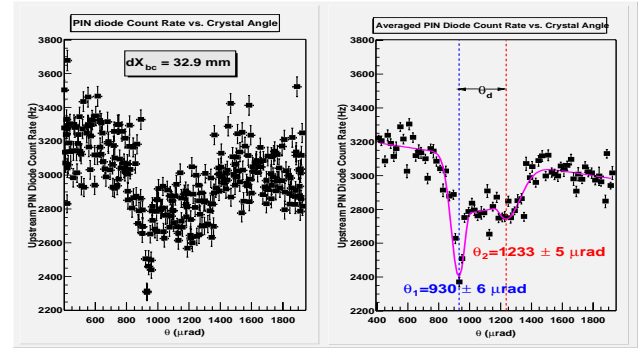


Figure 3: Crystal Scan with Au beam.

$$f(\theta) = \begin{cases} A_1 e^{-\frac{(\theta-\theta_1)^2}{2w_1^2}} + S\theta + T & : \theta < \theta_A \\ C(\theta - \theta_{ave}) + D + S\theta + T & : \theta_A < \theta < \theta_B \\ A_2 e^{-\frac{(\theta-\theta_2)^2}{2w_2^2}} + S\theta + T & : \theta_B < \theta \end{cases} \quad (2)$$

where $\theta_{1,2}$, $w_{1,2}$, and $A_{1,2}$ are the centers, widths, and amplitudes of the left and right dips, $\theta_{A,B}$ are the ends of the gaussians as determined by fit, θ_{ave} is the average of θ_1 and θ_2 , S and T are the slope and offset of the background, and C and D are determined by continuity at $\theta_{A,B}$.

Qualitatively, the data and the simulation agree well. There is an overall shift in the angular position between these data and the simulation. This is due to a difference of the miscut angle between the simulation and the crystal. The distance between the peaks is different. The simulation gives a distance θ_d of $440 \mu\text{rad}$ and the data shows a distance of $370 \mu\text{rad}$. This seems to indicate that the curvature of the crystal is not what was previously measured.

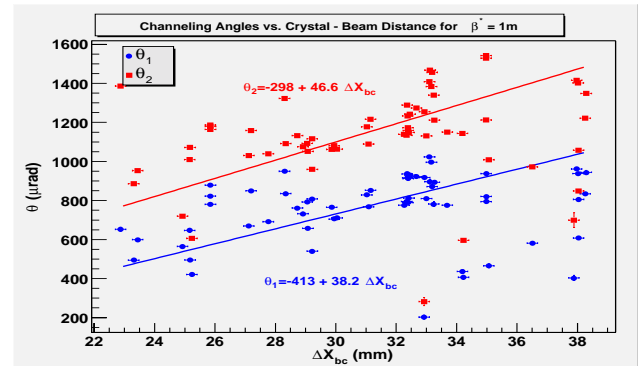

 Figure 4: Plot of channeling dip angles vs. distance from beam to crystal for gold beam, $\beta^* = 1$ m at PHENIX.

Figure 4 shows the location of the two channeling dips as a function of the distance from the beam to the crystal. According to our model, the slope of the graph is given by the Twiss parameters $-\alpha/\beta$, to the extent that dispersion is negligible. We expect $-\alpha/\beta = 23.5 \times 10^{-3} \text{ m}^{-1}$ for $\beta^* = 1$ m, the fits to the left and right dips yield $38.1 \pm 0.4 \times 10^{-3} \text{ m}^{-1}$ and $46.6 \pm 0.4 \times 10^{-3} \text{ m}^{-1}$ respectively.

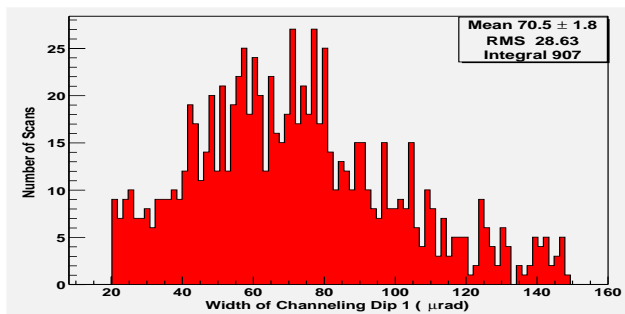


Figure 5: Distribution of widths of channeling dip 1

Figure 5 shows the width distribution of the large dip as determined from the fit. The mean width of $70.5 \pm 1.8 \mu\text{rad}$ is larger than the angular acceptance of $2\theta_c = 22 \mu\text{rad}$. At the location of the crystal, the beam is quite large ($\sigma = 5.3 \text{ mm}$, $\sigma_{x'} = -121 \mu\text{rad}$ for $\beta^* = 1\text{m}$) and converges to a downstream focus. The large angular spread of the beam may account for this extra width because the angular spread of the beam that hits the crystal is larger than $2\theta_c$.

Figure 6 shows the crystal channeling efficiency as seen from the upstream PIN diodes. The efficiency is defined as the ratio of the change in scattered particles due to channeling divided by the unchanneling rate of scattering. From the fit parameters we get $\epsilon = A_1/T$. The mean efficiency is 23%, about half of what is seen in Figure 2. Initially crystal defects were suspected. Using X-Ray diffraction, it was determined that the crystal quality was indeed very good [6]. So the small efficiency remains unexplained.

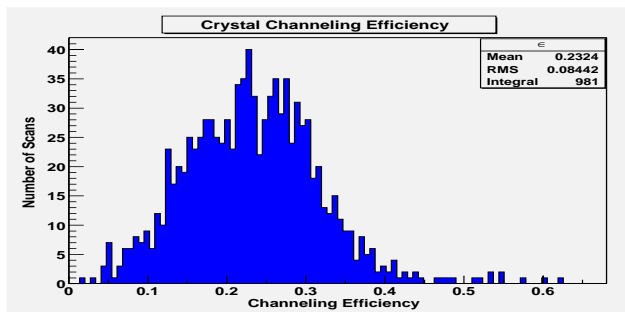


Figure 6: Distribution of efficiencies

7 CRYSTAL COLLIMATION

In order to measure the influence of the crystal on the experimental backgrounds, signals from the various experiments where recorded. The STAR detector, being 599 m downstream of the crystal collimator, was the most sensitive experiment. Figure 7 shows the effect of the crystal on the detector background. One can see that when the crystal is channeling the rates in the STAR Central Trigger Barrel (CTB) actually increase. This rate is considered background. Part of this is due to a misplacement of the scraper, so that channeled particles are not stopped. An-

other part may be halo caused by particles scattering from the crystal instead of channeling through it. When the copper scraper is properly placed with respect to the crystal, the extra background from the channeling is almost eliminated and there is sometimes a miniscule decrease in the CTB rates. In general, the crystal, when it was not channeling, caused increased background for the experiments [7].

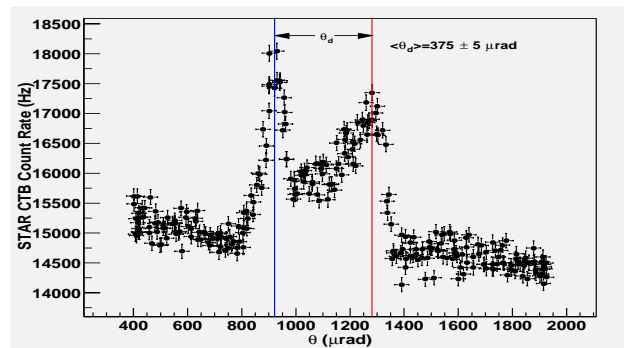


Figure 7: STAR CTB trigger rate during a crystal scan.

8 FUTURE PLANS

During the summer shutdown, various measurements will be made on the crystal to confirm the crystal quality. If the crystal reveals no defects it will be reinstalled in RHIC and used in the next run for more studies. These first experiments have shown that crystal collimation at RHIC has not yet reached an operational state and further experiments are needed to develop this exciting technology.

We thank Nuria Catalán-Lasheras for her assistance with the K2 code. We also thank Radoslav Adzic for his X-ray diffraction analysis of our crystals.

9 REFERENCES

- [1] T. Trenkler and J.B. Jeanneret., "The Principles of Two Stage Betatron and Momentum Collimation in Circular Accelerators" CERN Note: SL/95-03 (AP), LHC Note 312; M. Seidel. "The Proton Collimation System of HERA", Ph.D. thesis, Universität Hamburg, 1994 (DESY Report 94-103).
- [2] J. Lindhard. *K. Dan. Vidensk. Selsk. Mat.-Fys. Medd.* **34**, No. 14 (1965).
- [3] R. P. Fliller III, *et. al.* "The Two Stage Crystal Collimator for RHIC" Proceedings of the 2001 Particle Accelerator Conference, Chicago (2001).
- [4] V. Biryukov, "Crystal Channeling Simulation - CATCH 1.4 User's Guide", SL/Note 93-74(AP), CERN 1993.
- [5] T. Trenkler and J.B. Jeanneret. "K2. A software package for evaluating collimation systems in circular colliders." SL Note 94-105 (AP), December 1994.
- [6] Radoslav Adzic, private communication.
- [7] A. Drees, R. P. Fliller III, *et. al.* "RHIC Collimator Performance", these Proceedings. A. Drees. Backgrounds, collimation, gap cleaning. RHIC Retract 2002.